Relationship between Condensation Energy and Dimensionality of Bi-2212 superconductor

K. Okamura [a], M. Kiuchi [a], E. S. Otabe [a], T. Matsushita [a,1], T. Yasuda [a], S. Okayasu [b], S. Uchida [c], J. Shimoyama [c], K .Kishio [c],

[a] *Faculty of Computer Science and Systems Engineering, Kyushu Institute of Technology, 680–4 Kawazu, Iizuka 820–8502, Japan*

[b] *Japan Atomic Energy Research Institute, 2–4 Shirane, Tokai-mura, Naka-gun, Ibaraki, 319–1195, Japan*

[c] *University of Tokyo, 7–3–1, Hongo, Bunkyo-ku, Tokyo, 113–8656, Japan*

Abstract

The condensation energy which determines the pinning strength is estimated from the pinning property of the columnar defects for Bi-2212 superconductor in various doped states of oxygen. It is found that the condensation energy increases drastically with decreasing anisotropy parameter. In the low temperature region the condensation energy density of Bi-2212 increases abnormally with decreasing temperature and this suggests a drastic change in the superconductivity in the block layer.

Keywords: condensation energy density, anisotropy parameter, columnar defect,
PACS: 74.72.Hs, 74.60.Jg, 74.60.Ge

[1] Corresponding author.
Postal address: Faculty of Computer Science and Electronics, Kyushu Institute of Technology, 680-4, Kawazu, Iizuka 820-8502 Japan
Phone: +81-948-29-7661
Fax: +81-948-29-7661
E-mail address: okamura@aquarius10.cse.kyutech.ac.jp

Preprint submitted to VPP–30/ ISS2003

Submitted 27 October 2003

Revised 27 October 2003

1 Introduction

Weak pinning properties and low irreversibility field at high temperatures in two-dimensional Bi-2212 superconductor are attributed to its low condensation energy caused by the lack of superconductivity in thick block layers [1]. An improvement of pinning properties and a reduction in the anisotropy of the superconductor by oxygen doping are caused by enhancement of superconductivity in the block layer.

In a previous report [2], the relationship between condensation energy and dimensionality of Bi-2212 superconductor was discussed. The condensation energy was determined from estimated elementary pinning force of columnar defects nucleated by irradiation of nickel ions of 180 MeV for specimens prepared by KCl flux method. Specimens with the anisotropy parameter of $\gamma_a^2 = 9700 \sim 17000$ were investigated. The flux creep-flow theory was used to evaluate the virtual critical current density, J_{c0}, in the absence of flux creep from the observed critical current density, and the summation theory was used to estimate the elementary pinning force from J_{c0}. It was found that the condensation energy became large with increasing dimensionality of superconductor as expected.

In this study, we investigate the condensation energy of Bi-2212 specimens in a wider range of γ_a^2 than in the previous report. In addition, we use iodine ions of 200 MeV for the source to nucleate defects to examine if the previous results are reproducible. The critical current density and the irreversibility field are measured for such specimens and the condensation energy is estimated again.

2 Experimental

2.1 Specimens and measurement

Specimens were Bi-2212 single crystals prepared by floating-zone method. Typical size of the specimens was 2 mm × 1 mm × 10 μm and the c-axis was normal to a wide surface. Doped state of the specimens was controlled by changing a time and an oxygen partial pressure for annealing. In this study, an underdoped specimen was prepared to investigate the condensation energy in wider range of anisotropy parameter than in the previous report. These specimens were irradiated by iodine ions of acceleration energy of 200 MeV along the c-axis. The matching field for dose, B_ϕ, was 1.0 T. Iodine ions are expected to penetrate through the specimens to nucleate columnar defects of radius of about 3.0 nm. Specifications and critical temperature of the specimens are listed in TABLE 1. The critical temperature tends to decrease with doping, suggesting that the superconductor becomes less anisotropic.

The anisotropy parameter, γ_a, was estimated with the theoretical prediction, $\gamma_\mathrm{a}^2 = \phi_0/B_\mathrm{p}s^2$ [3], where B_p is a field at which a sharp peak of critical current density appeared, ϕ_0 is a flux quantum and s is a distance between superconducting layers. The values of the measured specimens are listed in TABLE 1 and the range in the present experiment is $\gamma_\mathrm{a}^2 = 8700 \sim 34500$.

To confirm the change in the anisotropy the lattice parameter, c, was measured by X-ray diffractmeter. Its values are listed in TABLE 1. c becomes smaller for a specimen with lower γ_a value, suggesting that the doped state can well be controlled by the annealing condition.

DC magnetization was measured in a magnetic field along the c-axis using a SQUID magnetometer and the critical current density, J_c, was determined from the magnetization hysteresis with an assumption of Bean's model. The irreversibility field was determined as a magnetic field at which J_c decreased to 1.0×10^7 A/m^2.

3 Theory

3.1 Summation Theory of Elemental Pinning Forces

We assume a columnar defect along the c-axis of radius, r_0, longer than the coherence length in the a-b plane, ξ_{ab}. The length of the defect is the same as the specimen thickness, t. The elementary pinning force of the defect for a parallel flux line is approximately given by

$$f_{\rm p} \simeq \frac{\pi B_{\rm c}^2 \xi_{ab} t}{4\mu_0}, \tag{1}$$

where $B_{\rm c}$ is the thermodynamic critical field.

Columnar defects are assumed to be distributed randomly but rather uniformly and the statistical theory is used for calculation of pinning force density. The nonuniform distribution of defects is approximated later by a wide distribution of an effective pin density in the pinning force density. According to the theoretical result [5], the virtual $J_{\rm c}$-value in the creep-free case is given by

$$J_{\rm c0} = \frac{\eta N_{\rm p}' f_{\rm p}}{B}, \tag{2}$$

where

$$N_{\rm p}' = \frac{\pi r_0^2 B B_\phi}{t\phi_0^2}, \tag{3}$$

is the effective pin density and η is a pinning efficiency describing a reduction from the direct summation. The statistical summation theory gives [5,6]

$$\eta = \frac{1-\alpha}{1+\alpha} \tag{4}$$

with

$$\alpha = \frac{(c^2+6c+1)^{1/2} - c - 1}{2c}, \qquad c = \frac{\phi_0}{\pi^2 r_0^2 B_\phi}. \tag{5}$$

In the above α is a relative threshold value of $f_{\rm p}$, and is always smaller than 1. The above result is considered to be the same as that in the so-called two-

dimensional pinning for thin superconductor because of strong synchronous pinning along flux lines by parallel columnar defects.

3.2 Flux Creep Theory

The current-voltage curve of a superconductor under a flux creep is determined by the pinning potential, U_0, which can be described in terms of J_{c0}. According to the collective flux creep theory, U_0 is given by [7]

$$U_0 = \frac{0.835 g^2 k_B J_{c0}^{1/2}}{\zeta^{3/2} B^{1/4}}; \qquad t > L, \tag{6}$$

where g^2 is a number of flux lines in a flux bundle, $\zeta \simeq 4$ for strong pinning centers and $L = (B a_f / \zeta \mu_0 J_{c0})^{1/2}$ is a longitudinal flux bundle size with a_f being a flux line spacing. The temperature and magnetic field dependency of J_{c0} at low fields is assumed to be given by

$$J_{c0} = A \left[1 - \left(\frac{T}{T_c} \right) \right]^m B^{\gamma - 1}, \tag{7}$$

where A, m and γ are pinning parameters. The electric field can be calculated based on the mechanism of flux creep and flow using the above pinning potential. The nonuniform distribution of columnar defects is approximated by a wide distribution of A describing a magnitude of J_{c0}:

$$f(A) = K \exp \left[- \frac{(\log A - \log A_m)^2}{2\sigma^2} \right], \tag{8}$$

where A_m is a most probable value of A, σ is a parameter representing a distribution width and K is a constant. Thus, the averaged current-voltage characteristic is calculated from

$$E(J) = \int_0^\infty E' f(A) \mathrm{d}A, \tag{9}$$

where E' is a local electric field determined from the mechanism of flux creep and flow. The details of this theoretical analysis are given in [8]. J_c is theoretically determined using the electric field criterion of 2.0×10^{-8} V/m for the magnetic measurement.

4 Results and Discussion

The observed J_c of four specimens at $T/T_c = 0.25$ before and after the ion-irradiation is shown in Fig. 1. It is found that J_c was about a few hundred times increased by the irradiation. Hence, J_c after the irradiation can be attributed to the pinning by columnar defects. Although a pronounced peak effect was observed before the irradiation, it disappeared after the irradiation. This suggests a change from two-dimensional vortex state to quasi-three-dimensional one at high fields due to strong parallel columnar defects. At high temperatures above 55 K J_c showed another peak in the field range of $B_\phi/3 \sim B_\phi$ as in Fig. 2. This is considered to be caused by enhancement of the probability of pinning by columnar defects due to a development of vortex coupling along the c-axis at a field of $B_\phi/3$ [9].

Fig. 3 shows temperature dependence of irreversibility field of four specimens before and after the irradiation. Before the irradiation the irreversibility field increased drastically with decreasing temperature below $T/T_c \simeq 0.35$ due to the dimensional crossover of flux lines. After the irradiation, the irreversibility field increased in the entire range of temperature and a plateau appears above $T/T_c \simeq 0.5$. At the same time the increase in the irreversibility field with decreasing temperature at low temperatures became moderate, and this also shows that the flux lines are in the quasi-three-dimensional state.

The pinning parameters, A_m, σ, m and γ are adjusted so as to get a good fit between the observed and calculated J_cs in the three-dimensional and quasi-three-dimensional vortex states above and below 40 K, respectively. These parameters are listed in TABLE 2. Using equations (1), (2) and (7), the condensation energy corresponding to the most probable value, A_m, is estimated at $B = 1$ T.

Fig. 4 shows the temperature dependence of the condensation energy. The present results are compared with the result on Y-123 [2]. In the high temperature region of $T/T_c > 0.5$, the condensation energy in Bi-2212 is much lower

than that in Y-123 and increases slightly faster than Y-123 with decreasing temperature. The condensation energy becomes larger with decreasing dimensionality of the superconductor. This is caused by an enhanced superconductivity in the block layer due to increased carrier density. In the low temperature region of $T/T_c < 0.4$, the condensation energy in Bi-2212 increases abruptly and approaches that in Y-123 with decreasing temperature. This anomalous increase in the condensation energy suggests an abrupt enhancement of superconductivity in the block layer. This explains the strong pinning and the insensitivity to thermal activation in Bi-2212 at low temperatures.

Fig. 5 shows the relationship between condensation energy and anisotropy parameter at $T/T_c = 0.8$. The previous results are also shown for comparison. The two sets of results fall on a single curve and clearly show the relationship between condensation energy and anisotropy parameter. This coincidence suggests a validity of the analysis described in this paper. It is found that the condensation energy depends strongly on the anisotropy parameter in some inverse power law. The thermodynamic critical field B_c of the present specimens at $T/T_c = 0.8$ is in the range of 10.4 mT $\sim$ 69.3 mT.

5 Summary

The condensation energy was estimated from the analysis of critical current density by columnar defects for Bi-2212 superconducting specimens in various doped states of oxygen. The condensation energy depends strongly on the anisotropy parameter in some inverse power law at high temperatures. At low temperatures the condensation energy increases abnormally with decreasing temperature, suggesting a drastic enhancement of superconductivity in the block layer.

References

[1] T. Matsushita, M. Kiuchi and H. Yamato, Adv. Cryog. Eng. Mater. **44** (1998) 647–654.

[2] L. Civale, A. D. Marwick, T. K. Worthington, M. A. Kirk, J. R. Thompson, L. Krusin-Elbaum, Y. Sun, J. R. Clem and F. Hotzberg, Phys. Rev. Lett. **67** (1991) 648–651.

[3] K. Okamura, M. Kiuchi, E. S. Otabe, T. Yasuda, T. Matsushita and S. Okayasu, The 11th International Workshop on Critical Current in superconductors (IWCC 11) To be published.

[4] V. M. Vinokur, P. H. Kes and A. E. Koshelev, Physica C **168** (1990) 29–39.

[5] M. Kiuchi and T. Matsushita, Adv. Supercond. **VIII** (1996) 497–500.

[6] T. Matsushita, Physica C **243** (1995) 312–318.

[7] N. Ihara and T. Matsushita, Physica C **257** (1996) 223–231.

[8] M. Kiuchi, K. Noguchi, T. Matsushita, T. Kato, T. Hikata, K. Sato, Physica C **278** (1997) 62–70.

[9] R. Sugano *et al*, Phys. Rev. Lett. 80 (1998) **2925**

Table 1
Specifications of specimens

specimen	condition of doping	T_c (K) before irradiation	T_c (K) after irradiation	γ_a peak field	c (nm) lattice parameter
A	$\sim$ 700℃ 0.1MPa(air)	88.7 K	87.0 K	187	3.0881
B	500℃ 0.1MPa(air)	90.3 K	88.9 K	148	3.0867
C	400℃ 0.09MPa(O_2)	87.0 K	84.6 K	127	3.0839
D	400℃ 0.21MPa(O_2)	78.8 K	78.4 K	93	3.0804

Table 2
Pinning parameters of specimens.

specimen	$T < 40$ K(quasi-3D vortex state) A_m	m	γ	σ^2	$T > 40$ K (3D vortex state) A_m	m	γ	σ^2
A	1.0×10^{11}	4.6	0.1	0.01	4.0×10^{10}	6.1	0.01	0.06
B	1.0×10^{12}	7.5	0.09	0.01	9.3×10^{10}	6.3	0.01	0.01
C	6.0×10^{11}	5.6	0.01	0.01	3.3×10^{10}	4.9	0.01	0.01
D	1.3×10^{12}	6.5	0.1	0.01	1.32×10^{11}	4.5	0.03	0.01

Figure 1 Critical current density of four specimens at $T/T_c = 0.25$.

Figure 2 Critical current density of specimen D at high temperatures.

Figure 3 Temperature dependence of irreversibility field of four specimens before and after the irradiation.

Figure 4 Temperature dependence of condensation energy.

Figure 5 Relationship between condensation energy and anisotropy parameter at $T/T_c = 0.8$.

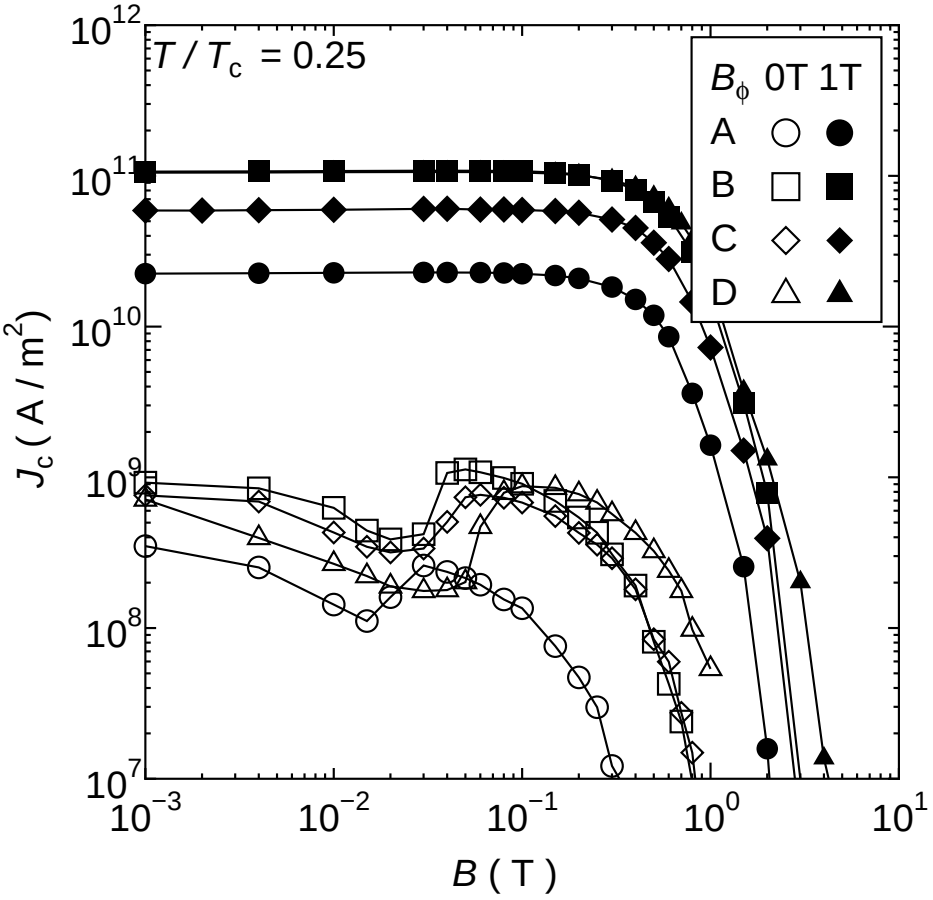

Figure 1 K .Okamura *et al.*

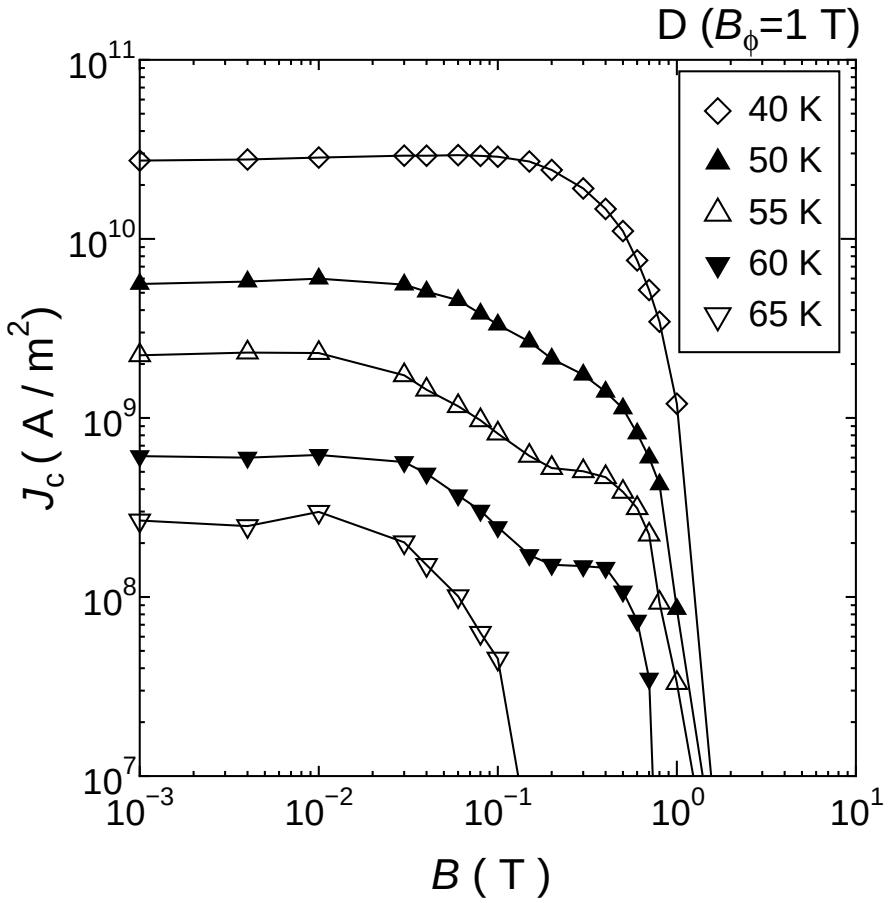

Figure 2 K .Okamura *et al.*

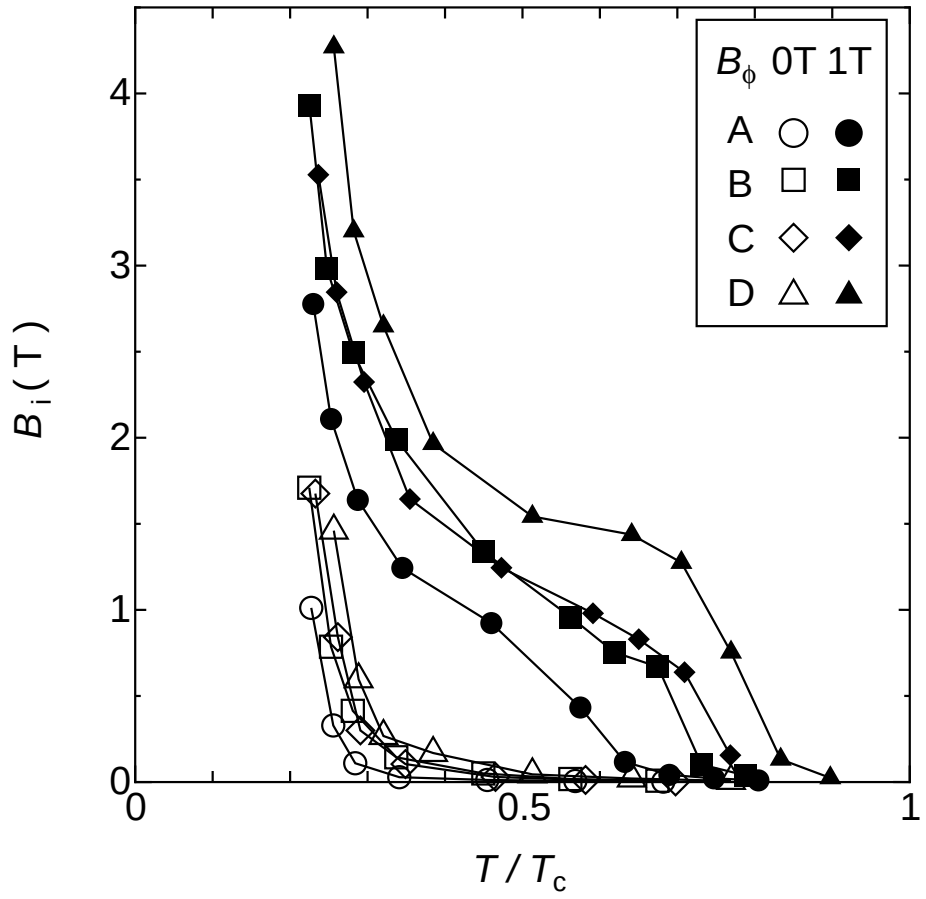

Figure 3 K .Okamura *et al.*

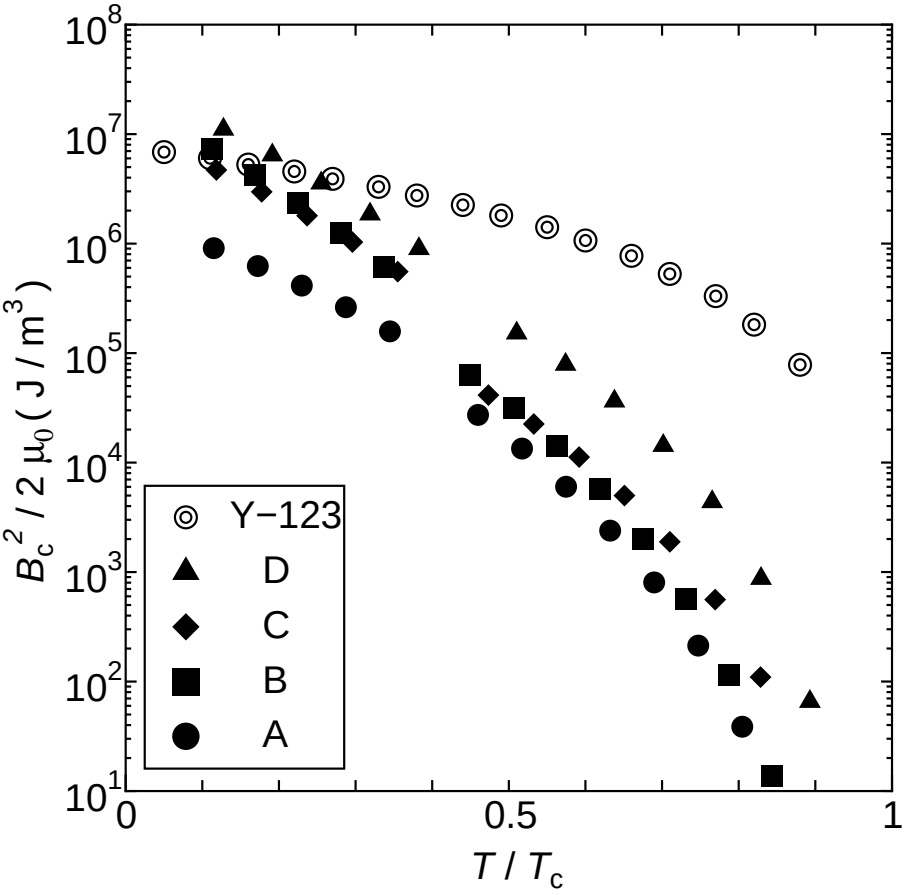

Figure 4 K .Okamura *et al.*

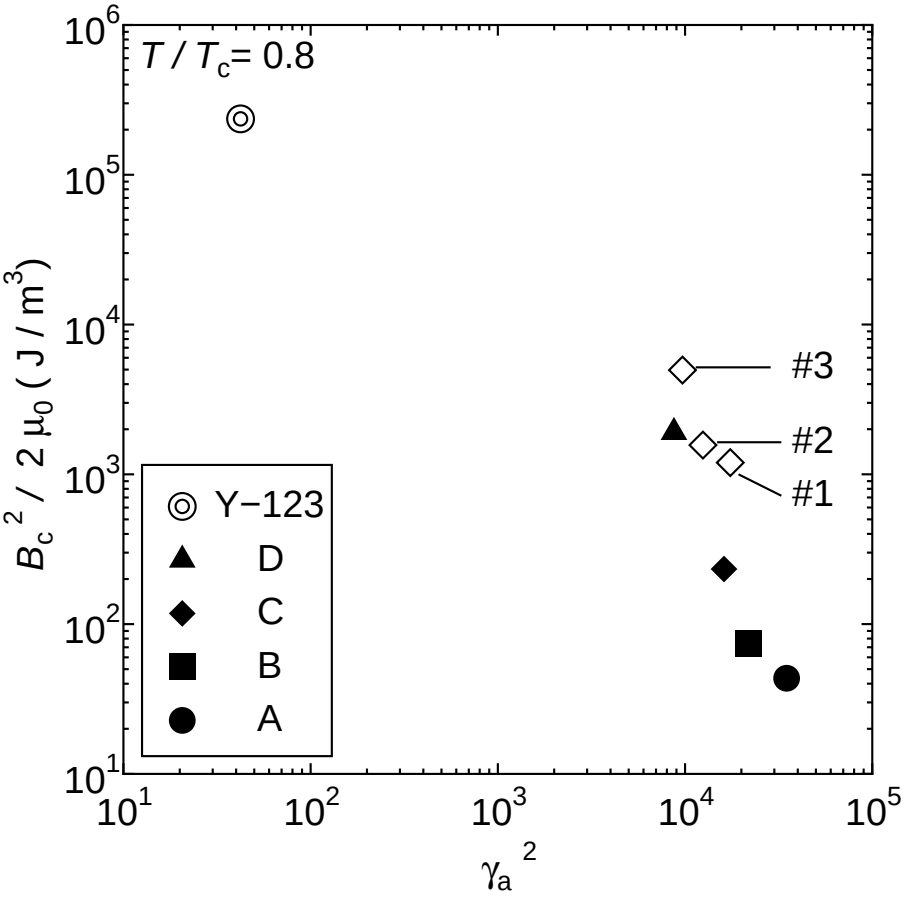

Figure 5 K .Okamura *et al.*